

The Ultraviolet Sky Surveys: Filling the Gap in our View of the Universe

Luciana Bianchi

© Springer-Verlag ••••

Abstract The GALEX mission is performing imaging and spectroscopic surveys of the sky at Ultraviolet wavelengths, and providing unprecedented sky maps in two UV bands, far-UV and near-UV, and catalogs of UV sources. I will describe the major surveys accomplished so far, and results in investigating the nature of the UV sources. The UV surveys, linked to a multi-wavelength archive, offer great sensitivity to detect and characterize several classes of astrophysical objects, such as low-redshift QSOs, star-forming galaxies, and white dwarfs (WD) in the Milky Way. Efforts towards obtaining a significant census of WDs from GALEX imaging data are described in particular. A dedicated, deep survey of nearby galaxies provides a snapshot of their recent star formation, shedding new light on the process of star formation and its modalities in different environments and conditions. Deep GALEX data revealed young stellar populations in extreme outskirts of spiral galaxies, previously thought to be stable against star formation given their low density. UV measurements for millions of nearby and distant galaxies map the history and probe the causes of star formation in the universe over the redshift range $z=0-2$.

Keywords astronomical data bases: surveys — astronomical data bases: catalogs — stars: white dwarfs — stars: early type — Galaxy: stellar content — galaxies: evolution — quasars: general — ultraviolet: general

Luciana Bianchi

Department of Physics and Astronomy, the Johns Hopkins University, Baltimore, USA

1 Introduction.

UV imaging and spectroscopic data with varied resolution and modes, for selected objects, have been provided over the last three decades by a variety of instruments, including several instruments on board the Hubble Space Telescope, and UV-dedicated telescopes, for example IUE and FUSE. Such data, disclosing important atomic species, has yielded unique results advancing our understanding of many astrophysical phenomena, from the interstellar and intergalactic medium to hot massive stars, mass loss phenomena, mass transfer and accretion, evolved stars, galaxy evolution and star formation, QSOs and black holes.

On the other hand, several sky surveys have been and are being performed in all other wavelength ranges, providing global views of the structure and evolution of the Galaxy and the Universe, and a “road map” for detailed investigations to be conducted by major instrumentation. The first comprehensive map of the sky in the UV has only begun to emerge with the launch of GALEX, in April 2003.

2 The GALEX data

The GALEX mission (Martin et al. 2005) is performing a series of imaging and spectroscopic sky surveys in two Ultraviolet bands, far-UV (FUV) and near-UV (NUV). The instrument consists of a 50 cm diameter modified Ritchey-Chrétien telescope providing a very wide field of view ($1.28/1.24^\circ$ [FUV/NUV] diameter) with good astrometric quality across most of the field, and a resolution of $\approx 4.2/5.3''$ [FUV/NUV] (Morrissey et al. 2007).

The GALEX data covers the wavelength range from 1344 Å to 2831 Å with two broad bands, the FUV passband (1344 - 1786 Å, $\lambda_{eff} = 1528$ Å) and the NUV band (1771 - 2831 Å, $\lambda_{eff} = 2271$ Å). A dichroic beam-splitter allows simultaneous observations in FUV and NUV.

The photometric system used in the GALEX archive, and in this paper, is based on the AB magnitude scale, defined as

$$m(AB) = -2.5 \times \log_{10} [\text{ergs cm}^{-2} \text{s}^{-1} \text{Hz}^{-1}] - 48.6$$

For GALEX, $m_{UV}(AB) = -2.5 \times \log CTR_{UV} + ZP$

where CTR_{UV} is the dead-time-corrected, flat-fielded count rate (counts s⁻¹), and the zero-points are $ZP_{FUV} = 18.82$ and $ZP_{NUV} = 20.08$. In some figures we also provide the Vega magnitude scale, to facilitate comparison with other work.

3 The Sky Surveys

3.1 AIS, MIS, DIS, UDIS

Imaging surveys are carried out with different depth and coverage. In the primary mission phase, which will be soon completed, four major imaging surveys were performed; their characteristics are summarized in Table 1. The All-sky Imaging Survey (AIS), has typically ~100-150 second exposures with a 5 σ NUV limiting magnitude of $m_{NUV}(AB) \sim 20.8$. The Medium Imaging Survey (MIS) has typically ~1500 second exposures and limiting magnitude of $m_{NUV}(AB) \sim 22.7$ (Morrissey et al. 2007). The Deep Imaging Survey (DIS) reaches $m_{FUV}/m_{NUV} \sim 24.8/24.4$ for a typical exposure of 30,000 seconds. However, the exposure level of some deep fields (including e.g. XMMLSS, CDFS, Lock-00, Groth) reaches over 70,000 seconds (Ultra-deep survey).

The photon-counting delay-line detectors provide great linearity over a wide dynamic range, and the low detector background allows significant measurements down to the sky background level. The detector electronics begins to incur in non-linearities for magnitudes brighter than about 15. The effects are shown by Morrissey et al. (2007) and are discussed further by Bianchi et al. (2008). To some extent the non-linearity can be corrected and slightly brighter objects can be recovered. Due to the bright limits, it is currently impossible, for example, to survey with GALEX the Magellanic Clouds. Aside from several successfully observed peripheral fields, detector shut-down events occurred when trying to observe even

UV-faint (based on rocket data) fields in inner regions of these galaxies. It may be possible to push the bright limits later on in the mission. The All-Sky Imaging Survey (AIS) aims at covering as much as possible of the sky, however pointings must avoid bright stars, and therefore the coverage is not entirely contiguous, especially towards the Galactic plane. Fig. 1 shows the sky coverage for the three main imaging surveys as of May 2007. Table 1 compiles the basic characteristics and statistical properties of the resulting catalogs.

3.2 Nearby Galaxies Survey, NGS

The Nearby Galaxies Survey (NGS, Bianchi et al. 2003) performed dedicated imaging of hundreds of nearby galaxies, with a typical depth of 27.5 mag/arcsec², providing sensitivity to low levels of star formation (roughly $10^{-3} M_{\odot} \text{Kpc}^{-2}$). While the dedicated NGS observations amounted to about 300 pointings (see Table 1), the program leveraged on the MIS survey observations of comparable sensitivity, and the AIS survey greatly extends the number of fields but with shorter exposures. The NGS (for the primary phase of the mission) has been described e.g. by Bianchi et al. (2003); a first atlas containing UV images and light profiles of 1034 galaxies larger than $D_{25} = 1'$, observed in the first two years of the GALEX mission with exposures of at least 1000 sec, is presented by Gil de Paz et al. (2007). In total, with any level of exposure, over 40,000 galaxies within 100 Mpc (velocity $\leq 7000 \text{ km s}^{-1}$) are now included in the GALEX imaging surveys, out of about 50,000 galaxies listed in Hyperleda database within such velocity limit (Thilker, priv. comm.).

3.3 Spectroscopic surveys

In addition to the imaging surveys, GALEX also provides slitless spectroscopy in both FUV and NUV bands simultaneously, with a spectral resolution of $\lambda/\Delta\lambda \sim 200/90$ [FUV/NUV]. Nested spectroscopic surveys with different sky coverage and depth are under way, and the first spectral datasets are also available from the public archive, although the calibration for the spectroscopic data is still preliminary at this time.

3.4 Extended Mission Surveys

The GALEX “extended mission phase” will begin in 2008, with several new surveys planned. The Time Domain Survey will provide time-repeated

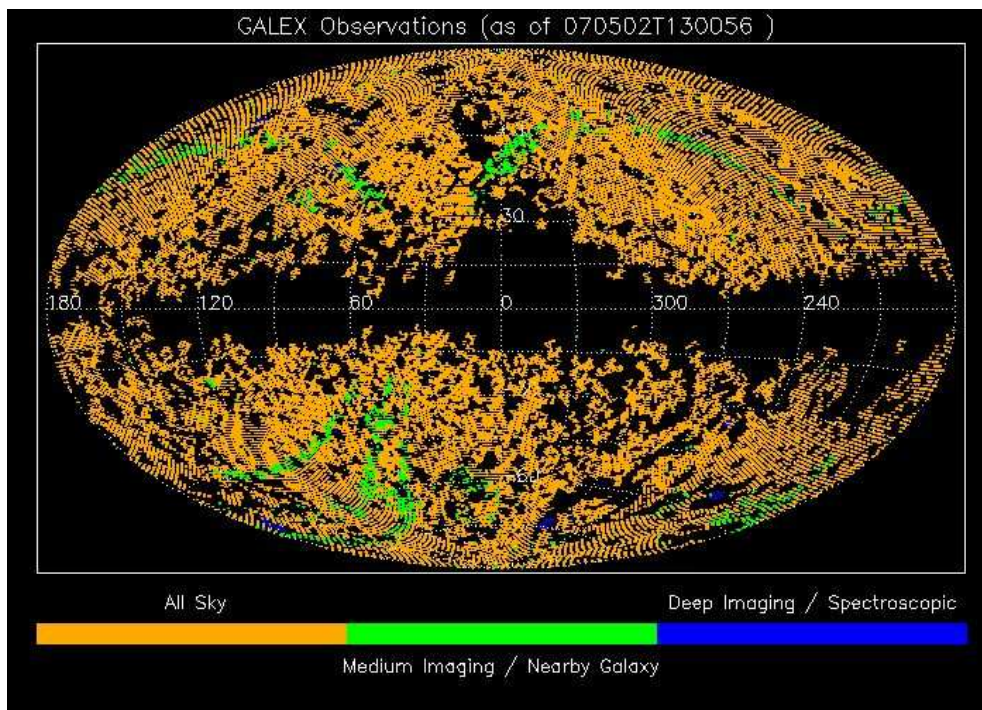


Fig. 1.— The sky coverage of the GALEX major imaging surveys as of May 2, 2007: AIS (orange), MIS (green), DIS (blue). The map is in Galactic coordinates.

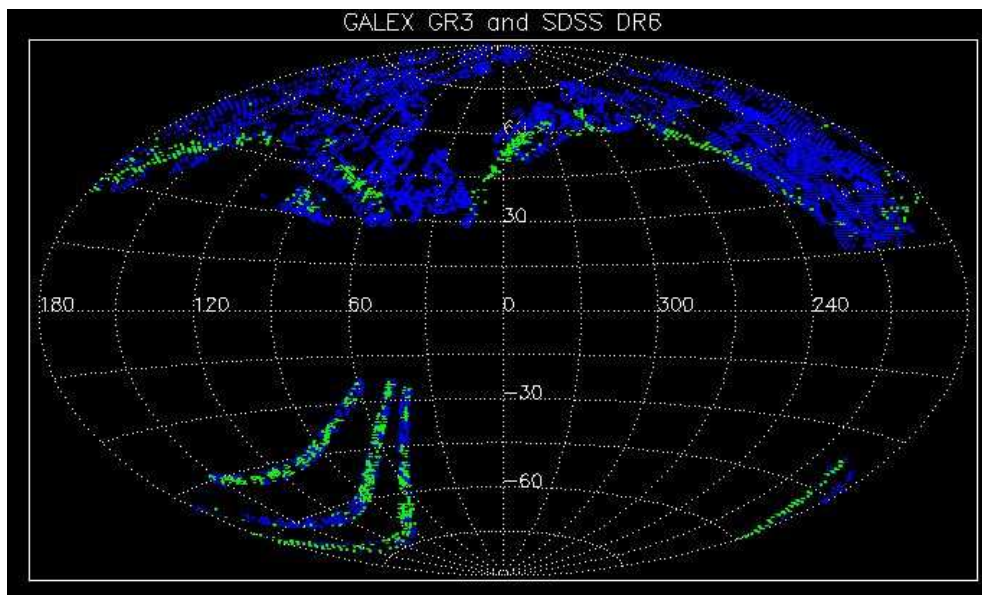


Fig. 2.— The portions of the GALEX imaging surveys AIS (blue) and MIS (green) released in the public data release GR3, overlapping with the SDSS data release 6 (DR6). Both GR3 and DR6 releases are now publicly available. Map in Galactic coordinates.

measurements of selected fields for variability studies, either with dedicated observations or by an optimized cadence of the repeated observations in fields where deep exposures are to be achieved. The extended mission may also largely match the SDSS “SEGUE” survey, as well as include the Galactic Cap Survey, extended spectroscopic, MIS and DIS surveys, and others. Finally, the GALEX mission also includes a Guest Investigator program.

4 The Ultraviolet Sky

What objects do we see when we look at the sky in the Ultraviolet? Which objects are most numerous at different depths? What are the UV-brightest objects in the sky? How far does GALEX detect UV-emitting stars in the Milky Way? What is the weakest star formation we can measure? Which galaxies and QSOs are seen in the UV surveys?

Here we provide a description of the content of the GALEX catalogs, and a characterization of the UV sky, by a statistical classification of the UV sources. To this aim, we consider a subset of the GALEX surveys which overlaps with the footprint of the Sloan Digital Sky Survey (SDSS) most recent data release (DR6). The SDSS project (York et al. 2000) is mapping one fourth of the sky in five broad optical bands: *u g r i z* using a dedicated 2.5m telescope with a wide-field of view and a 0.5-meter telescope for photometric calibration. The SDSS data provide photometry in five optical bands for the matched UV sources, and optical spectra for a subset of them, useful to verify the classification based on photometric criteria.

We limit the analysis to the sources in the inner 0.5° radius of the GALEX field of view, for best astrometric and photometric quality. With this restriction, the total area of unique coverage (i.e. excluding overlap among different fields) matched between the GALEX GR3 release and SDSS DR6 is 3390° for AIS and 573° for MIS, out of a total GALEX unique coverage of $12128/792^\circ$ (AIS/MIS) in the GR3 (using a 0.5° radius and excluding the GR3 small supplemental releases). The area of overlap has been computed with the algorithm described by Bianchi et al. (2006). The sky coverage presented here is almost tenfold larger than the data used by Bianchi et al. (2007), and allows us to explore trends with Galactic latitude of the UV sources and the extinction.

We followed procedures similar to Bianchi et al. (2007, 2006, 2005a) to construct a “clean” catalog of matched GALEX-SDSS sources. For a meaningful classification and analysis, the sample must be restricted to objects with good photometry. The effects of applying error cuts to the sample (decreasing the number of sources, and limiting the depth to brighter magnitudes) are illustrated quantitatively in Figs 2-4 of Bianchi et al. (2007). In particular, imposing good measurements in the FUV band, reduces the sample to about 10% of the total NUV detections, and mostly eliminates intermediate temperature stars and medium-to-high redshifts QSOs and galaxies: compare Fig.6 to Fig.5 of Bianchi et al. (2007) to appreciate the effect. We eliminated multiple GALEX entries for the same objects (all repeated observations are entered in the GALEX database), we matched the catalog of “unique” GALEX sources to the SDSS catalog (using $4''$ initial match radius), and flagged the UV sources with more than one optical counterpart within the match radius (the SDSS psf, about $1.4''$, is smaller than the GALEX psf, resulting in some closeby objects to not be resolved in the UV). Such sources (few percent) will not be used in the classification analysis because their colors are composite, but must be taken into account statistically.

5 Classification of the UV sources

Figs 3 to 5 show the colors (combined UV-optical) of the GALEX sources compared to template colors for major classes of astrophysical objects. The model colors are described by Bianchi et al. (2007), and show the expected *locus* of stars (supergiants, main sequence, WDs) of varying T_{eff} , QSOs of varying redshift, and galaxies of different types at varying age. Reddening effects due to interstellar dust are also shown. The sources are also distinguished by their spatial extent, using the SDSS images information (psf $\sim 1.4''$): the unresolved sources (blue dots in the figure) are mostly stars and QSOs, while the extended sources (black dots) are mostly star-forming galaxies. This is confirmed by spectroscopic classification for a large subset of the sample (several thousand). In the deeper MIS catalog (Figs 4 and 5), we see also some Elliptical galaxies detected at old ages, due to the “UV-upturn” emission. At the AIS depth, the number of Milky Way objects and extra-galactic objects is similar, but the density

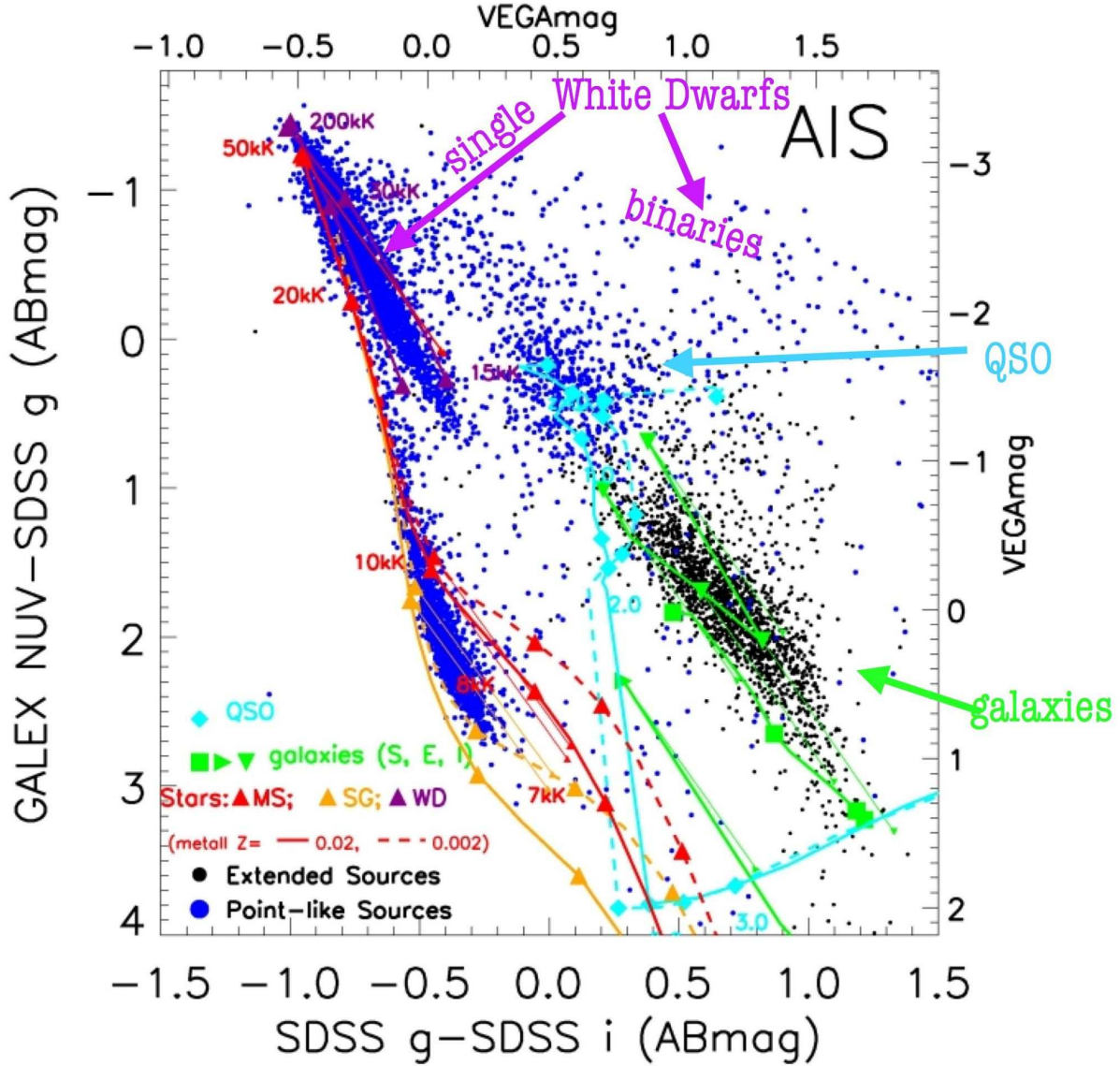


Fig. 3.— UV sources from our matched GALEX-GR3-AIS / SDSS-DR6 sample: blue dots are point-like sources, black dots are extended sources (mostly galaxies). Model colors for stars with $\log g=3$ (yellow), 5 (red), 7 and 9 (purple) are shown for different T_{eff} . Most point-like hot sources are bracketed by the $\log g=7$ and $\log g=9$ stellar sequences, and they are WD or sub-dwarfs. Note the QSOs color locus for $z=0.1-1.6$ (and a cluster of QSO points) well separated from stars and galaxies. Another very interesting feature is an arc-like distribution of point-like sources (blue dots), which are mostly stellar binaries containing a hot WD and a cooler star. Thin-line arrows show extinction effects for $E(B-V)=0.5$.

Table 1 Major GALEX Imaging surveys (primary mission) and coverage to date.

| Survey | Typical Exp. (sec) | limiting mag (AB) FUV / NUV | limiting flux F_{λ} FUV / NUV | #sources/ \square° (average) | # fields in GR3 | #Sources in GR3 | #Fields as of May 2007 |
|------------------------------|-----------------------|--------------------------------|--|--|--------------------|--------------------|---------------------------|
| All Sky Imaging Survey (AIS) | 100 | 19.9 / 20.8 mag | $5.2/1.1 \cdot 10^{-16}$ ergs $\text{cm}^{-2} \text{s}^{-1} \text{\AA}^{-1}$ | 5000 | 15721 | 85M | 27925 |
| Medium Imaging Survey (MIS) | 1500 | 22.6 / 22.7 mag | $4.3/1.8 \cdot 10^{-17}$ ergs $\text{cm}^{-2} \text{s}^{-1} \text{\AA}^{-1}$ | 13000 | 1017 | 13.5M | 1673 |
| Deep Imaging Survey (DIS) | 30000 | 24.8 / 24.4 mag | $5.7/3.8 \cdot 10^{-18}$ ergs $\text{cm}^{-2} \text{s}^{-1} \text{\AA}^{-1}$ | 30000 | 122 | 3M | 151 |
| Nearby Galaxies Survey (NGS) | 1500 | 27.5 mag/ \square° | $4.7/2.2 \cdot 10^{-19}$ ergs $\text{cm}^{-2} \text{s}^{-1} \text{\AA}^{-1} \square^{\circ-1}$ | n.a. | 296 | see text | 307 |

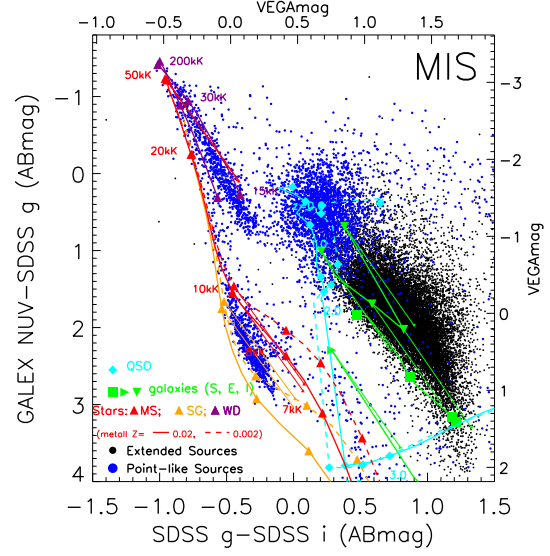


Fig. 4.— Same as in the previous figure, for the MIS sample. The lower number of hot stars (with respect to Fig. 3) is due to the MIS smaller area coverage, but the density of objects per square degree is higher, because the MIS extends to fainter magnitudes (see Table 1 and Fig. 7). At fainter magnitudes, the relative number of extragalactic objects (QSOs and galaxies) respect to the MW stars increases rapidly: compare to the previous figure.

of QSOs and galaxies increases rapidly at fainter magnitudes, as can be seen at a glance by comparing color-color diagrams for AIS and MIS (see also Bianchi et al. 2007, 2006).

6 A census of hot WDs in the Milky Way

Figs 6, 7 and 8 show the characteristics of the hot WD candidates, extracted from the GALEX photometric catalog described in section 4, from the matched GALEX GR3 and SDSS DR6 datasets. This sample ($\sim 15,000$ WDs) represents a factor of up to ~ 10 increase in area coverage over the work of Bianchi et al. (2007). Our selection of WD candidates, based mainly on the FUV-NUV color, includes stellar objects hotter than approximately 18,000 K (the color cut corresponds to a slightly different T_{eff} 's depending on the star's gravity). The depth of the MIS sample corresponds, for example, to the magnitude of a hot WDs (50,000-100,000 K) with radius as small as $0.04R_{\odot}$ at a distance of 20 Kpc, in absence of extinction (see Bianchi et al. 2007). Therefore we

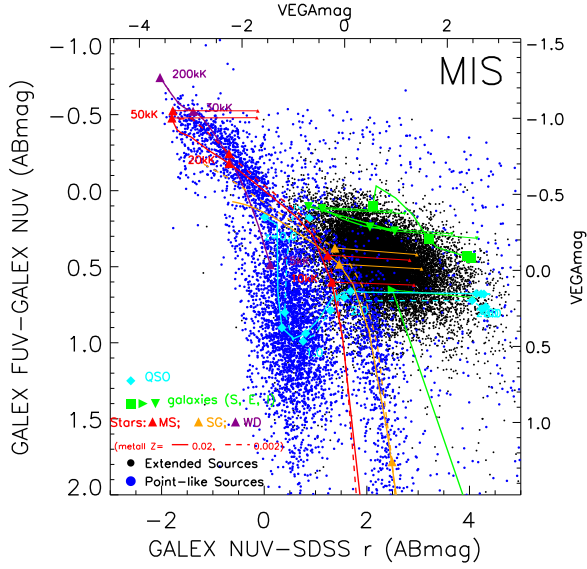


Fig. 5.— Same as in previous figures. Note how the QSOs at redshift $z \sim 1$ separate well from both stars and galaxies in this color-color diagram. Note also a sequence of cooler stars, and again a distribution of blue dots with “hot-WD” FUV-NUV color but red optical colors (binaries). Unlike the previous two diagrams, in this color combination the reddening effects and T_{eff} color variations are completely disentangled.

expect the MIS samples to be fairly conclusive at high galactic latitudes where extinction is small. The ~ 2 mag brighter AIS samples would be correspondingly limited to closer objects, or distant objects with larger radii/luminosities.

7 Galaxies and QSOs

Figs 3, 4 and 5 illustrate that low redshift ($z < 1.6$) QSOs separate quite well from galaxies and stars in color space when GALEX bands are included. The advantages with respect to using optical colors only are discussed by Bianchi et al. (2005c). The only stellar objects partly sharing the QSO *locus* in the color-color diagrams are some types of stellar binaries and in particular objects with mass-transfer disk or hot spots such as Cataclysmic Variables (CVs), which are rare. The color *locus* of the bluest galaxies is contiguous or slightly overlapping with the QSOs. In this regard, we point out that in our diagrams we use the automated classification (from the optical pipeline) of the sources

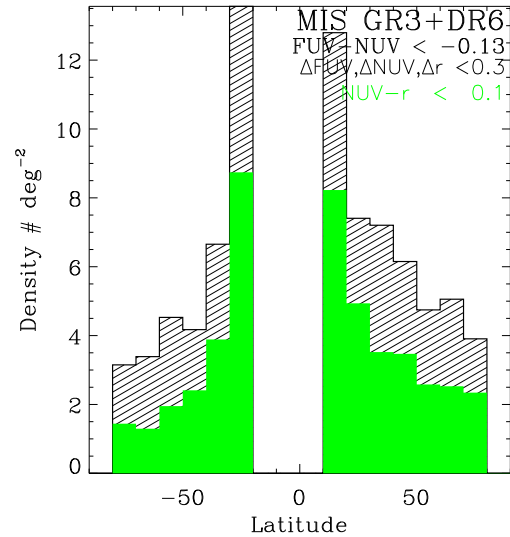
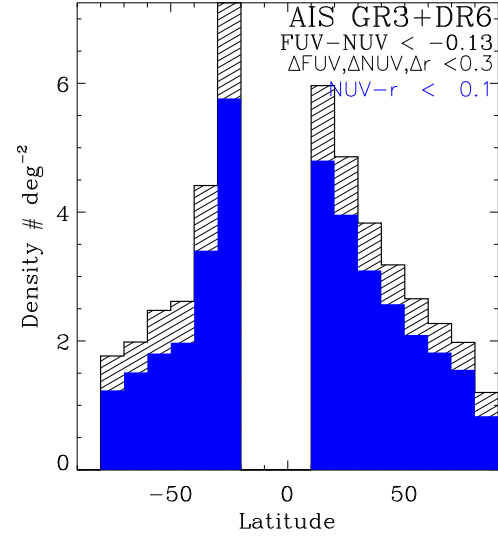


Fig. 6.— Density of WD candidates from AIS (top, blue) and MIS (lower panel, green) as a function of Galactic latitude, from the current GALEX samples, all magnitudes. Solid color histograms are the “single WD” candidates (Fig. 3), dashed histograms include also sources with WD-like UV color and redder optical colors: these are candidate binaries including a WD and a cooler star, but contain also a high number of extragalactic objects at the fainter magnitudes. Note the different scale used, because MIS reaches fainter magnitudes therefore the counts are higher. The bins have varying statistical significance according to the available coverage in different latitude slices (see Fig. 2). Extinction effects have not been taken into account in these plots, yet the MW structure is emerging with variations by over a factor of five.

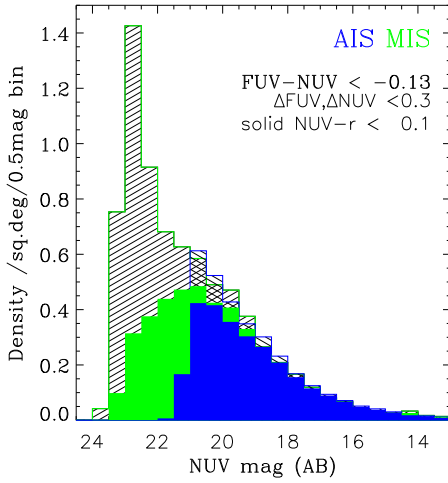


Fig. 7.— Density of WD candidates (AIS and MIS) as a function of magnitude (all latitudes). Symbols as in previous figure. The AIS sample has larger sky coverage, thus better statistics. It agrees with the MIS counts until it becomes incomplete, and drops at ~ 21 mag. The “single-WD” sample (solid colors) has a purity of over 90%, while the increase of the dashed histograms at faint magnitudes is due to contamination by extragalactic objects (see e.g. Bianchi et al.2007)

in either “point-like” or “extended”. This is an objective criterion but obviously the result depends on the contrast between the central source and the underlying host galaxy. Such contrast is not well characterized at redshift around 1, and deeper optical imaging of our GALEX-selected QSOs is under way to provide new insight. When we plot on the color-color diagrams the QSOs confirmed as such by optical spectroscopy (a sample will be shown in a forthcoming paper), we see that the majority constitutes the cluster of blue dots (point-like sources) over the low- z QSO templates in our figures. A small number extends towards the contiguous galaxy locus, although their location may just indicate high reddening. More interestingly, we find a number of QSOs with UV flux much higher than canonical QSO SEDs. We will discuss these UV-bright QSOs in a forthcoming paper. Fig. 11 of Bianchi et al. (2007) shows the GALEX-selected QSO sample (from the GR1 data release), compared to the SDSS QSO catalogs. A larger sample (about 30,000 QSOs) extracted from the catalog described in this paper will be published elsewhere. However, because the QSO density does not depend on Galactic latitude (save for local extinction in sight-lines close to the Galactic

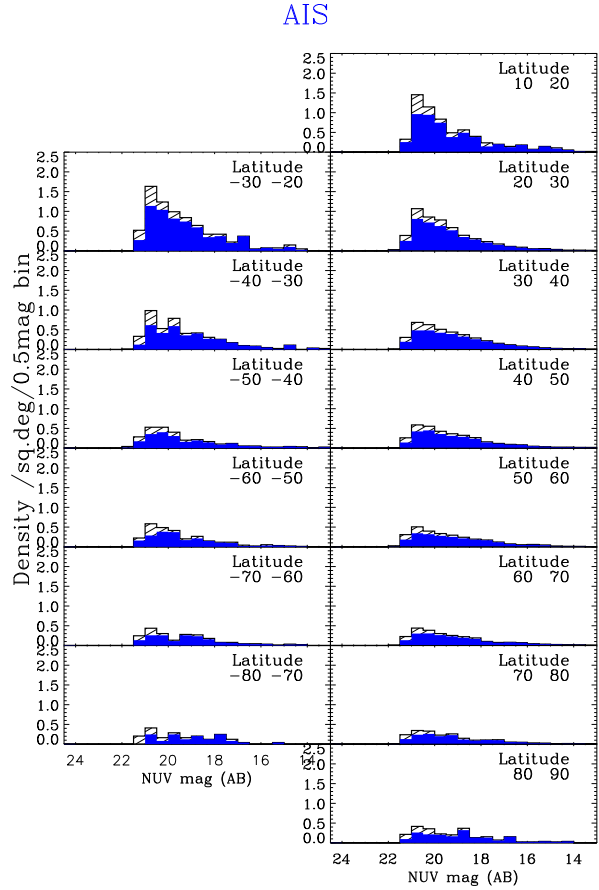


Fig. 8.— Density of WD candidates (AIS sample) as a function of magnitude, for slices of 10° Galactic latitude. Uncorrected for interstellar extinction.

plane), one can usefully compare the QSO density of Bianchi et al (2007) with the density of WD candidates shown in this paper (Fig. 7) to appreciate the relative increase of extragalactic objects versus Milky Way stars at fainter magnitudes. The estimated contamination of the QSO sample by WD and CVs is $< 15\%$ for QSOs with redshift around 1. This fraction is confirmed by a subsample of UV sources with optical spectroscopy.

As for normal galaxies, GALEX provides an unprecedented overview of the star-forming regions in nearby galaxies. The FUV and NUV bands, and the derived UV color, are very sensitive to ages up to a few hundred million years (Fig.9). In Local Group galaxies, GALEX images revealed unambiguously an important number of star-forming sites which are inconspicuous at other wavelengths, and had not been previously studied, in spite of many excellent past and recent optical

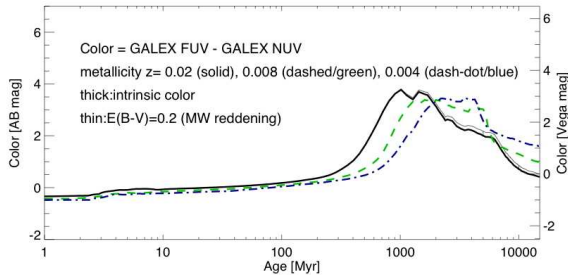


Fig. 9.— The GALEX FUV-NUV color for a single-burst population (SSP), shown for three metallicity values. The GALEX broad-band colors were computed using Padua SSP models, kindly provided by A. Bressan.

surveys including broad-band and H_α data (e.g. Massey et al. 2006, 2007). A follow-up program (Bianchi et al) with HST imaging at high resolution is under way to study the resolved stellar populations in the GALEX-selected sites.

Many unique, and unexpected, discoveries were enabled by GALEX’s sensitivity and wide field of view. The combination of these two factors led for example to the discovery of star formation in outer regions of some spiral galaxies, extending out to 4-5 times the optical radius (R_{25} or R_{HII}). Such regions were previously believed to be stable against star formation due to the extremely low gas density. More details about the extended UV-disks (XUVD) are given in a contributed paper in these proceedings (Bianchi, Thilker et al). Other important measurements enabled by these data are the detection of perturbation-triggered star formation in the “tidal tails” of interacting galaxies. UV emission, both diffuse and in knots (possible dwarf galaxies in formation?) is detected along “tails” on scales up to ~ 100 Kpc. The GALEX color and flux provides age-dating for the star formation, a useful comparison to the dynamical times to understand the induced process. Examples are shown in Fig. 10. See also e.g. Hibbard et al. 2005, Xu et al. 2005, Neff et al. 2005, Bianchi et al. 2005b.

Last but not least, one of the primary science goals of the GALEX mission was to measure the history of star formation in the recent universe ($z=0-2$, 80% of the life of the universe). UV measurements (eventually for millions of galaxies) provide the relation between star formation and UV luminosity, and extinction by interstellar dust, and are used to reconstruct the star formation back in time from the present day, as a function of galaxy mass and other characteristics (e.g. Martin et al. 2007, Salim et al. 2007). Combined with optical

and IR data, UV measurements are the subject of numerous such studies, too many to be mentioned here. We refer to a dedicated ApJ Supplement issue (173/2, Dec. 2007) for a collection of papers based on GALEX data.

Acknowledgements Most of this paper is based on work done in collaboration with B. Efremova and D. Thilker, who also prepared some of the figures, and J. Herald. S. Heinis offered useful discussions. I am also extremely grateful to the GALEX SODA team, for the excellent mission operation, support and data flow which is producing an unprecedented gold mine of (currently over 100 million) UV sources. Related papers are available at the author’s web site: <http://dolomiti.pha.jhu.edu>.

GALEX (Galaxy Evolution Explorer) is a NASA Small Explorer. We gratefully acknowledge NASA’s support for construction, operation, and science analysis of the GALEX mission, developed in co-operation with the Centre National d’Etudes Spatiales of France and the Korean Ministry of Science and Technology.

Facilities: GALEX, Sloan

References

- Bianchi, L., et al.. 2007, ApJS, 173, 659
- Bianchi, L., et al.. 2006, *The UV Universe: Stars from Birth to Death*, eds A.I.Gomez de Castro & M.Barstow, in press
- Bianchi, L., et al.. 2005a, ApJ, 619, L27
- Bianchi, L., et al.. 2005b, ApJ, 619, L71
- Bianchi, L., et al.. 2005c, AAS 207, 133.13
- Bianchi, L., et al.. 2003, *The Local Group as Astrophys. Laboratory*, eds M.Livio & T.Brown, STScI, p.10
- Gil de Paz, A., et al. 2007, ApJS, 173, 185
- Hibbard, J., et al.. 2005, ApJ, 619, L87
- Martin, C., et al. 2007, ApJS, 173, 415
- Martin, C., et al. 2005, ApJ, 619, L1
- Massey, P., et al. 2006, AJ, 131, 2478
- Massey, P., et al. 2007, AJ, 133, 2393
- Morrissey, P., et al. 2007, ApJS, 173, 682
- Neff, S., et al. 2005, ApJ, 619, L91
- Salim, S., et al. 2007, ApJS, 173, 267
- Thilker, D., et al. 2007, ApJS, 173, 538
- Thilker, D., et al. 2005, ApJ, 619, L79
- Xu, K., et al. 2005, ApJ, 619, L95
- York, D. et al. 2000, AJ, 120, 1579

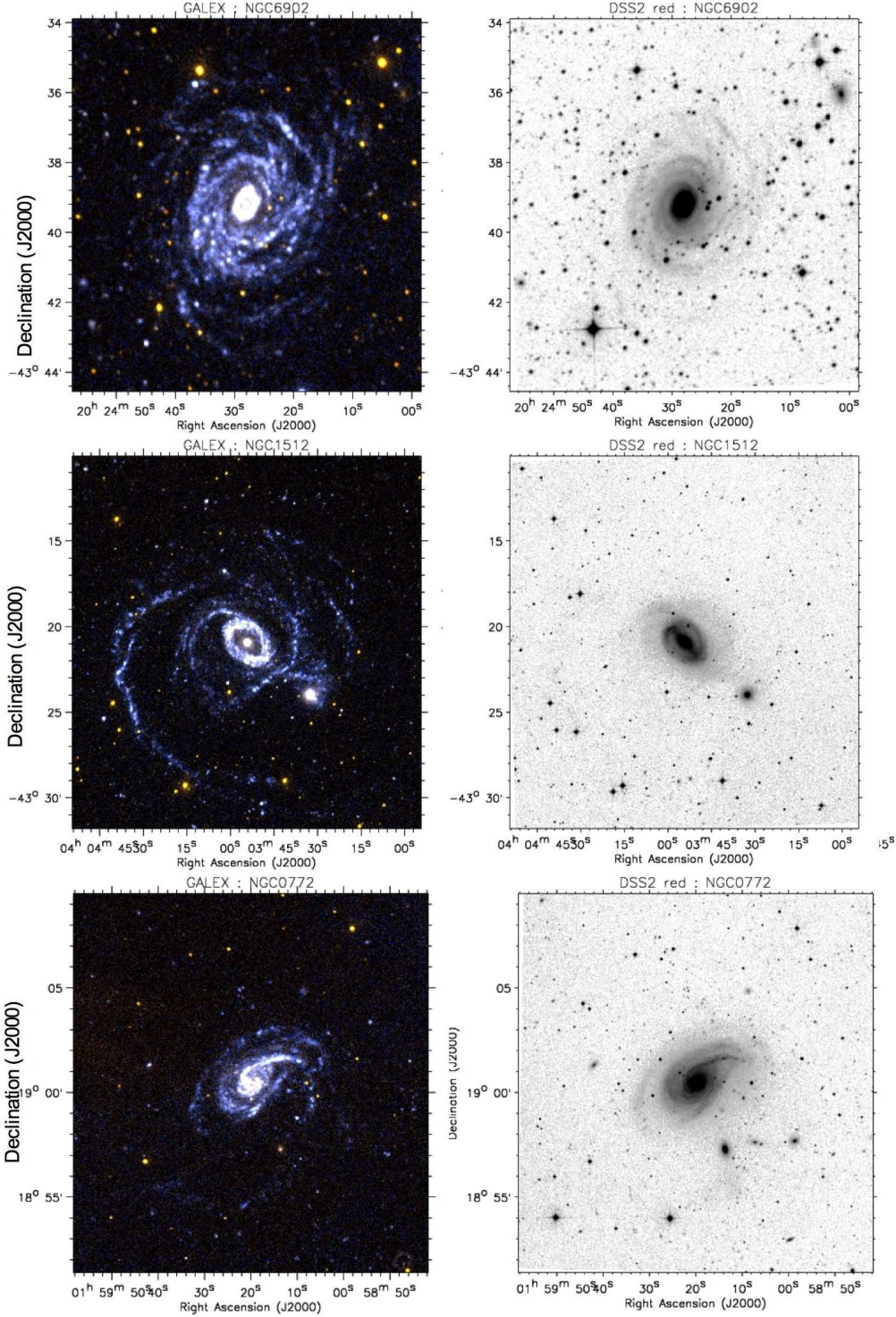


Fig. 10.— FUV (blue) and NUV (yellow) composite color images (left) and optical red images (right) of three nearby galaxies. In the interacting pairs, tidal tails are seen on very large scales, and low levels of star formations are detected. Figures adapted from Thilker et al. (2007). See also Bianchi, Thilker et al. in these proceedings.